

Contents lists available at [SciVerse ScienceDirect](http://SciVerse ScienceDirect)

## Taiwan Journal of Ophthalmology

journal homepage: [www.e-tjo.com](http://www.e-tjo.com)

## Review article

Choroidal imaging by spectral domain-optical coherence tomography<sup>☆</sup>Lihteh Wu<sup>\*,a</sup>, Natalia Alpizar-Alvarez*Instituto de Cirugia Ocular, San José, Costa Rica*

## ARTICLE INFO

## Article history:

Received 26 November 2012

Received in revised form

26 January 2013

Accepted 29 January 2013

Available online 7 March 2013

## Keywords:

age-related macular degeneration

central serous chorioretinopathy

choroidal thickness

diabetic retinopathy

enhanced depth imaging

glaucoma

inherited retinal diseases

intraocular tumors

macular holes

OCT

Vogt-Koyanagi-Harada syndrome

## ABSTRACT

Despite the fact that the choroid plays an important role in the structure and function of the eye, it has not been studied in detail *in vivo*. Improvements in optical coherence tomography (OCT) imaging technology allow the routine imaging of the choroid and deep optic nerve structures in most patients. As with any new technology, it needs validation in both healthy and diseased eyes. Reproducible measurements of choroidal and lamina cribrosa thickness are possible. Several variables such as age, axial length, and time of day, affect choroidal thickness and must be taken into account when interpreting data on choroidal thickness. Lamina cribrosa thickness appears to be affected by age as well but other factors need to be determined. Choroidal thickness may be used to differentiate between central serous chorioretinopathy (CSC), polypoidal choroidal vasculopathy (PCV) and exudative age-related macular degeneration (AMD). Enhanced depth imaging-optical coherence tomography (EDI-OCT) of the choroid may detect tumors not detectable by ultrasound. Studying the choroid may help us gain insight into the pathogenesis of several diseases such as AMD, CSC, glaucoma, posteriorly located choroidal tumors, and PCV among others.

Copyright © 2013, The Ophthalmologic Society of Taiwan. Published by Elsevier Taiwan LLC. All rights reserved.

## 1. Introduction

The choroid plays an important role in the structure and function of the normal eye. Most of the ocular blood flow is accounted for by the choroidal circulation. In fact, the choroid has one of the highest blood flow rates in the entire body. In addition, the choroid supplies oxygen and nutrients to the outer retinal layers.<sup>1</sup> An understanding of the pathophysiological changes that occur in the choroid is of paramount importance in understanding disease of the posterior segment of the eye.

Despite advances in imaging technology, adequate visualization of the choroid is still lacking. Traditional imaging modalities used to study the choroid such as indocyanine green angiography (ICGA) and B scan ultrasonography have limitations with regard to image resolution and measurement accuracy.

Optical coherence tomography (OCT) is a non-invasive, noncontact transpupillary imaging modality that has revolutionized

ophthalmic clinical practice. It utilizes light to image tissue using low coherence interferometry.<sup>2</sup> Time domain OCT does not image the posterior choroid and sclera adequately. Current commercially available spectral domain (SD)-OCT systems may be modified to allow adequate choroidal imaging.

## 2. OCT choroidal imaging

There are a few strategies that may improve choroidal OCT imaging, namely bringing the choroid closer to the zero delay line using SD-OCT using a light source with a longer wavelength or using swept source OCT.

During SD-OCT imaging, a beam of low coherence light from a superluminescent diode is split through a beam splitter into a sample and a reference beam. Light from the sample beam is directed toward the tissue of interest, in this case the posterior segment of the eye, and depending on the composition of the internal tissue structures, the sample beam will be reflected towards the detector with different echo time delays. The reference beam is reflected from a reference mirror towards another detector. Both reflected beams of light are compared and combined into an interference pattern by a modified Michelson interferometer, called the spectral interferogram or spectrometer.<sup>2,3</sup> Fourier equations transform this spectral interferogram into two OCT

<sup>☆</sup> Presented in part at the Taiwan Academy of Ophthalmology Spring Meeting, March 31, 2012, Taipei, Taiwan.

\* Corresponding author. Apdo 144-1225 Plaza Mayor, San José, Costa Rica.

E-mail address: [LW65@cornell.edu](mailto:LW65@cornell.edu) (L. Wu).

<sup>a</sup> Lihteh Wu has received honoraria for lectures from Heidelberg Engineering.

mirror images. The screen of the OCT instrument only depicts one of these images. By convention, the image depicted places the vitreous at the top of the screen and the choroid towards the bottom of the screen. In this position, the vitreous is at the peak of the OCT sensitivity curve and closer to the zero delay line.<sup>4,5</sup> When an OCT instrument is positioned closer to the eye, the inverted mirror image is obtained and the choroid approaches the zero delay line. This inverted mirror image has more information from the deep choroid than the normal noninverted image (Fig. 1). Eye tracking and image averaging capability are important features that improve the signal-to-noise ratio with resulting improvement of visualization of the choroid. In order to obtain the best quality image, it is important to try to keep the image straight and to keep the inverted image close to the top of the screen. Spaide and collaborators<sup>4,5</sup> coined the term enhanced depth imaging (EDI) to describe this novel choroidal OCT imaging technique using the Spectralis (Heidelberg Engineering, Heidelberg, Germany) OCT system. The most recent Spectralis software version makes EDI even more user friendly by incorporating EDI into the scanning protocols. Therefore, all the operator needs to do is press the EDI button, and the software automatically inverts the image. Image averaging, eye tracking, high-speed scanning, and low speckle noise produce high-quality choroidal images with the EDI mode in the Spectralis OCT.

Most commercially available OCT systems use a light source of approximately 800 nm, which penetrates the choroid and sclera poorly. Both the photoreceptor and retinal pigment epithelium (RPE) layers scatter the 800-nm light signal, resulting in a weak signal from the choroid (Fig. 1). An investigational OCT device that uses a light source of 1060 nm has been developed. The longer wavelength of the light source permits a higher penetration and visualization of the choroidoscleral interphase allowing accurate measurement of the choroidal thickness.<sup>6</sup>

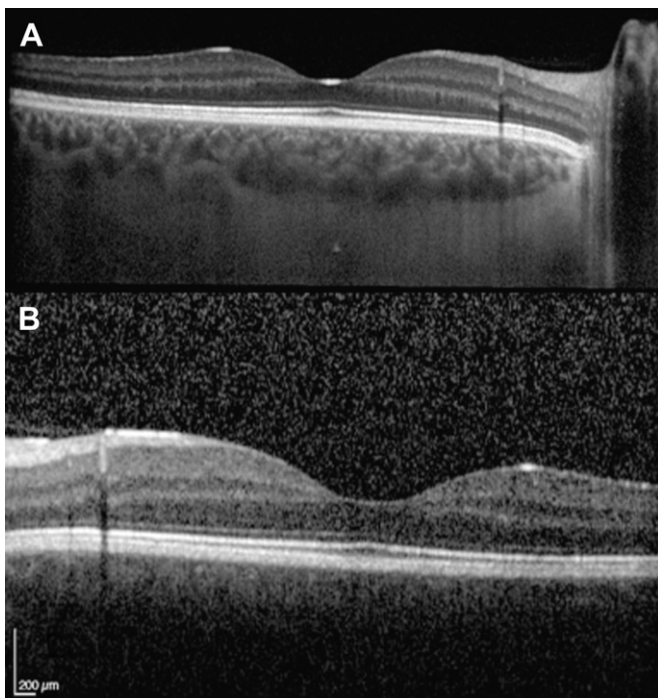


**Fig. 1.** Comparison between conventional Spectralis optical coherence tomography (OCT) scanning and enhanced depth imaging (EDI) OCT scanning of the macula of the same patient. (A) EDI-OCT showing choroidal details and the choroidal scleral interphase. (B) Conventional OCT showing no choroidal details.

Swept source OCT is another device that uses a frequency swept laser with a narrowband light source that is rapidly tuned over a broad optical bandwidth that enables the measurement of interference at different optical frequencies or wavelengths sequentially over time.<sup>7</sup> No spectrometer or line camera is needed for the Fourier transformation. This increases the imaging speed up to 300,000 axial scans per second and allows a deeper penetration of the sampling beam.

Choroidal imaging and thickness measurements have been reported with several commercially available OCT systems including the Cirrus (Carl Zeiss Meditec Inc, Dublin, CA), Topcon 3DOCT 2000 (Topcon Corporation, Tokyo, Japan), Optovue RTVue (Optovue Inc, Fremont, CA), Biotigen (Biotigen Inc, Research Triangle Park, NC, USA) and the Heidelberg Spectralis.<sup>4,5,8</sup> Not all machines are created equally. For instance, the Cirrus OCT system lacks eye tracking ability, and hence the averaging of the images is less likely to improve the signal-to-noise ratio. Furthermore, with Cirrus, it is unclear where the image is placed within the sensitivity curve.<sup>9</sup> As a matter of fact, with the Cirrus it is important not to bring the choroid to the zero delay line since image inversion with the Cirrus software results in images of very low quality.<sup>8</sup> Lin et al<sup>10</sup> compared the choroidal thickness, visualization of the choroido-scleral junction, and visibility of the large outer choroidal vessels across several SD-OCT systems using upright and inverted images. They reported that the most favorable modes to visualize choroidal details were Spectralis in either EDI or inverted mode, Biotigen in the inverted mode and Cirrus in upright mode. They also stated that choroidal thickness cannot be compared between machines because of different conversion factors.<sup>10</sup>

### 3. Choroidal thickness in normal eyes

There is currently no automated segmentation software that is commercially available to measure the choroidal thickness. Therefore, once the EDI-OCT image is obtained, the choroidal thickness needs to be measured manually by using calipers to measure the distance from the outer border of the RPE to the inner surface of the sclera (Fig. 2). Investigators have recently unveiled an

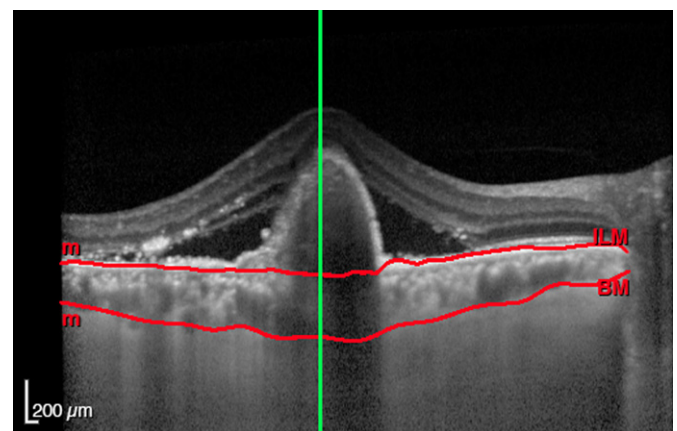


**Fig. 2.** There is currently no automated segmentation software available to measure the choroidal thickness in the Spectralis machine. Therefore, once the EDI-OCT image is obtained, the choroidal thickness needs to be segmented semi-automatically using the built-in automated retinal segmentation software on the Spectralis SD-OCT. By using the software of the Heidelberg spectralis we have manually moved the lines of the ILM to the RPE and the RPE to the choroidoscleral junction. The retinal boundary reference lines placed by the built-in automated segmentation software were moved to the choroidal boundaries. BM = Bruch's membrane; EDI-OCT = enhanced depth imaging-optical coherence tomography; ILM = internal limiting membrane; RPM = retinal pigment epithelium; SD-OCT = spectral domain-optical coherence tomography.

automated segmentation of the choroid for Cirrus OCT. This software automatically separates the choriocapillaris from the choroidal vasculature.<sup>11</sup> Additional studies need to be performed to validate the use of this software.

There is considerable inter-individual variability in choroidal thickness.<sup>12</sup> Choroidal thickness measurements in normal subjects appear to be highly reproducible.<sup>5,13,14</sup> A change of  $>32\ \mu\text{m}$  in subfoveal choroidal thickness probably exceeds interobserver variability.<sup>13</sup> Chlhaablani et al<sup>15</sup> have shown that measurements of choroidal volume by manual segmentation using the built-in automated retinal segmentation software on Spectralis SD-OCT are highly reproducible and have a low level of variability. Prior to utilizing choroidal thickness as a parameter to monitor disease conditions, normal physiological parameters that affect choroidal thickness need to be identified.

Choroidal thickness exhibits regional variations across the posterior pole. It varies according to macular location. Margolis and colleagues<sup>4</sup> performed EDI-OCT of the posterior pole with 7 sections within a  $5 \times 30$  degree area centered at the fovea, with 100 scans averaged for each section. They measured the choroidal thickness in this area and reported that the choroid was thinnest nasally, thickest subfoveally, and thinner temporally. The inferior macular choroid was also thinner than the superior macular choroid.<sup>4,8</sup> In another study, choroidal volumes were calculated using an investigational device with a 1050-nm light source.<sup>12</sup> They used an Early Treatment of Diabetic Retinopathy Study (ETDRS)  $6\ \text{mm} \times 6\ \text{mm}$  grid that was superimposed in the posterior pole to delineate 9 macular subfields. The thickest choroid was found in the outer superior subfield, whereas the thinnest choroid was located in the outer nasal subfield. In addition, they reported a greater correlation between the choroidal thickness and the distance from the optic nerve head rather than the distance from the fovea. The authors of this study suggest that the optic nerve head might be a better reference point than the foveal center to study regional differences in choroidal thickness. The only exception was inferonasal section of the disc, where the most pronounced choroidal thinning was present.<sup>12</sup> Ikuno et al<sup>16</sup> have hypothesized that the presence of a vascular

watershed zone and the embryonic location of the optic fissure closure are responsible for this choroidal thinning. Ouyang et al<sup>12</sup> support this hypothesis and propose that this choroidal thinning inferonasal to the disc is a relative coloboma that all healthy eyes exhibit as a remnant of normal embryological development.

Age is another variable that needs to be taken into account when comparing choroidal thickness.<sup>4,12</sup> In normal eyes, progressive choroidal thinning occurs over time at a rate of  $1.56\ \mu\text{m}$  per year in the subfoveal area<sup>4</sup> (Fig. 3). The mean subfoveal choroidal thickness in normal eyes has been reported to be  $287\text{--}332\ \mu\text{m}$ . The difference between studies is probably because of the difference in mean age in these studies.<sup>5,12,13</sup>

The axial length and refractive status also appear to influence choroidal thickness. There is an inverse relation between myopia and choroidal thickness<sup>12,17</sup> (Fig. 4). Choroidal thickness decreased almost  $32\ \mu\text{m}$  for every 1 mm increase in axial length.<sup>12</sup> In highly myopic eyes ( $>6\ \text{D}$ ) and no observable fundus changes, subfoveal choroidal thickness decreased by  $12.7\ \mu\text{m}$  for each decade of life and by  $8.7\ \mu\text{m}$  for each diopter of myopia.<sup>17</sup> Subfoveal choroidal thickness is an important predictor of visual acuity in highly myopic eyes.<sup>18</sup>

Gender might play a role in choroidal thickness. Li et al<sup>19</sup> reported that women have a thinner choroid than men. In contrast, Chen et al<sup>20</sup> did not find any gender related differences in choroidal thickness.

Since a large portion of the choroid is comprised by vascular structures, it is conceivable that hemodynamic variables affect choroidal thickness. In one study, the total choroidal blood flow and the subfoveal choroidal blood flow did not appear to affect subfoveal choroidal thickness.<sup>21</sup> In contrast, a recent study showed that ocular perfusion pressure might be associated with subfoveal choroidal thickness in young healthy individuals.<sup>22</sup> Acute changes in systolic blood pressure induced by exercise did not affect subfoveal choroidal thickness either.<sup>23</sup>

Diurnal fluctuations in choroidal thickness have recently been described.<sup>24,25</sup> The choroid appears to be thicker at night and thinner during the day. These fluctuations appear to be associated with age, axial length, refractive error, and systolic blood pressure.<sup>24</sup>

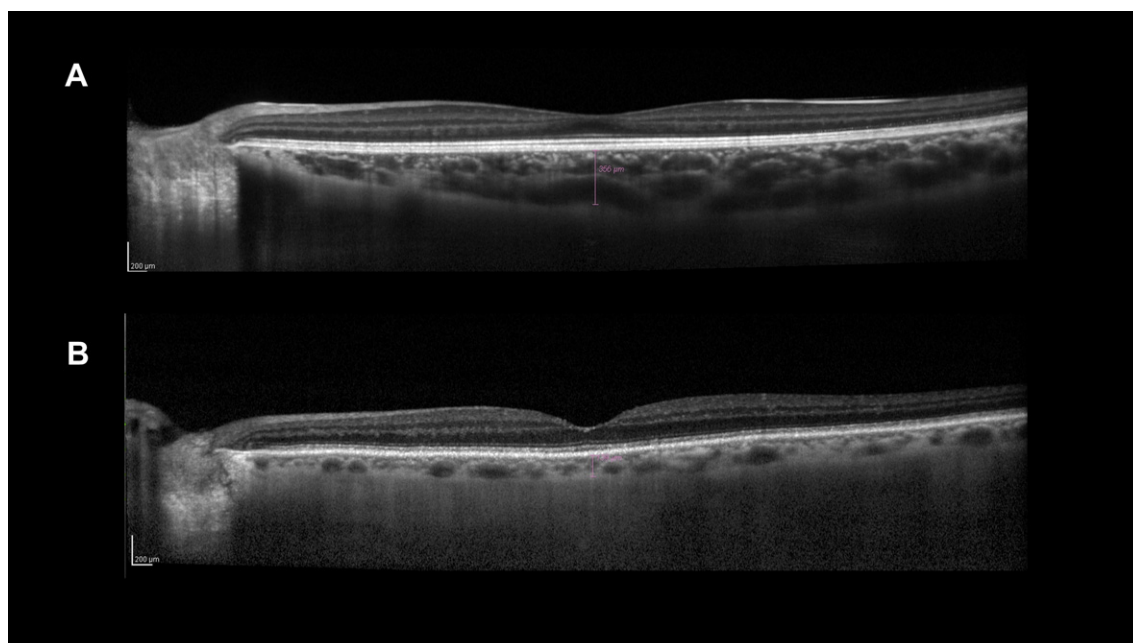


**Fig. 3.** Comparison between enhanced depth imaging-optical coherence tomography scans in two patients of different ages. (A) A 12-year-old boy with a subfoveal choroidal thickness of  $356\ \mu\text{m}$ . (B) An 83-year-old woman with subfoveal choroidal thickness of  $139\ \mu\text{m}$ .



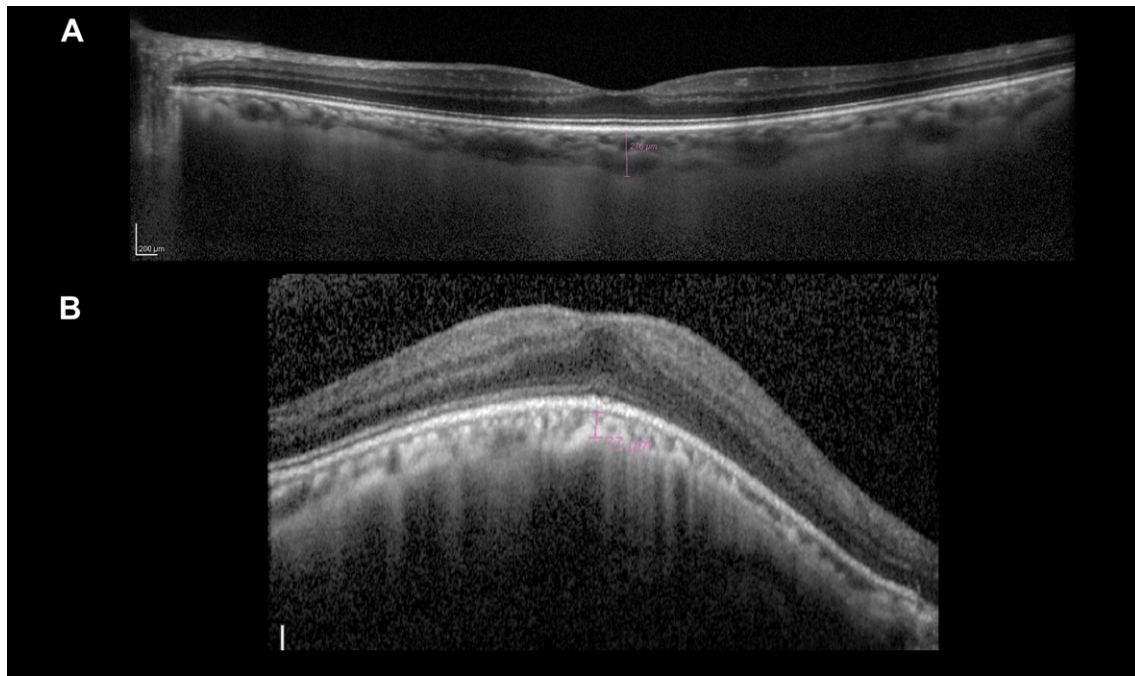


**Fig. 4.** Comparison of enhanced depth imaging-optical coherence tomography scans according to refractive status. (A) A 38-year-old woman with no refractive error and a subfoveal choroidal thickness of 276  $\mu\text{m}$ . (B) A 36-year-old woman with 8 D of myopia and a subfoveal choroidal thickness of 77  $\mu\text{m}$ .

#### 4. Clinical applications

McCourt et al<sup>26</sup> compared the subfoveal choroidal thickness in eyes with different ophthalmic pathologies and compared it to a normal cohort. They reported that eyes with glaucoma, diabetic retinopathy, and age-related macular degeneration (AMD) had a significantly thinner choroid than normal patients. However, when age was taken into account as a confounding variable, the

differences disappeared underscoring the effect that aging plays in determining choroidal thickness.

#### 5. Central serous chorioretinopathy

Central serous chorioretinopathy (CSC) is thought to arise from choroidal vascular hyperpermeability.<sup>27</sup> Several studies have used EDI-OCT and swept source SD-OCT to demonstrate that in CSC, the

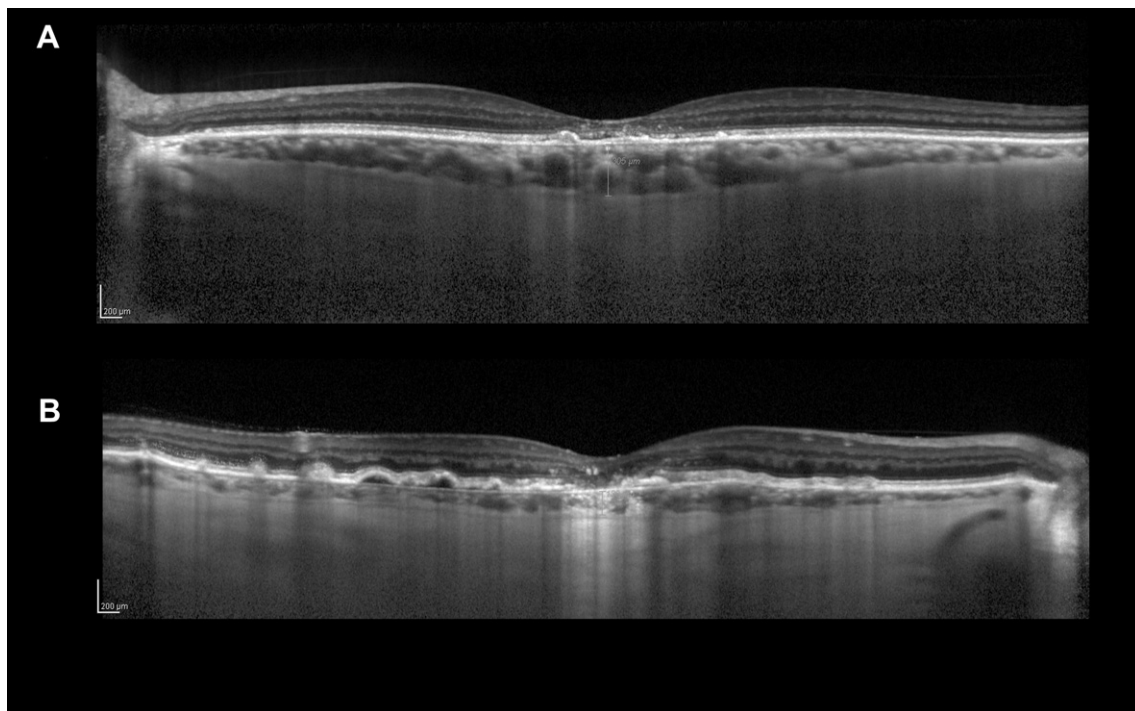


**Fig. 5.** Differentiation between AMD and CSC using choroidal thickness. In general, patients with CSC tend to have a thicker choroid. Conversely, patients with AMD tend to have a thinner choroid. (A) A 67-year-old woman with active CSC. Subfoveal choroidal thickness is 305  $\mu\text{m}$ . (B) A 71-year-old woman with exudative AMD and a subfoveal choroidal thickness of 139  $\mu\text{m}$ . AMD = age-related macular degeneration; CSC = central serous chorioretinopathy.

choroidal thickness increases<sup>9,28–31</sup> (Fig. 5). Jirarattanasopa et al<sup>30</sup> constructed choroidal macular maps by manually segmenting choroidal thickness and then using the bundled automated software to measure the volume between the segmented lines. They showed that the increased choroidal thickness seen in CSC was a diffuse phenomenon throughout the macular area and not limited to focal points.<sup>30</sup> Interestingly enough, choroidal thickness is usually increased in both the affected and the fellow eye.<sup>28,32</sup> This is in agreement with the indocyanine green angiography (ICGA) findings that show bilateral vascular choroidal hyperpermeability even in the eyes without subretinal fluid.<sup>33</sup> This lends further credence to the hypothesis that an increased choroidal hydrostatic pressure plays an important role in the pathogenesis of this disease. Following the successful treatment of active CSC with either full- or half-fluence photodynamic therapy, the choroidal thickness was found to decrease.<sup>29–31</sup> In eyes treated successfully with laser photocoagulation, leakage resolved, but the choroidal thickness remained high.<sup>29,30</sup> EDI-OCT of the choroid has documented that sildenafil citrate increases choroidal thickness and thus may be a risk factor for CSC.<sup>34,35</sup> Alternatively, sildenafil might be used as a treatment in those conditions that would benefit from an increased choroidal blood flow.<sup>35</sup>

## 6. Age-related macular degeneration

The pathogenesis of the disease process in age-related macular degeneration (AMD) is not completely understood. Multiple environmental, dietary, and genetic factors appear to play a role in this condition. Theories from chronic inflammation to ischemia have been proposed.<sup>36–38</sup> With aging, there is an increasing lipid deposition in the sclera, choroid, and Bruch's membrane.<sup>39</sup> According to Friedman,<sup>37</sup> this deposition leads to an increased resistance to choroidal blood flow and decreased choroidal perfusion, which may contribute to the development of AMD. High resolution OCT imaging of the choroid may shed some light in this regard.

There have been conflicting reports with regard to choroidal thickness in patients with early AMD.<sup>40,41</sup> In one study, choroidal thickness was found to be similar between 16 Welsh eyes with early AMD and 16 eyes in an age-matched control.<sup>40</sup> In another study of 17 Korean eyes with early AMD, choroidal thickness was less than that of the age-matched control eyes.<sup>41</sup> Manjunath et al<sup>42</sup> reported that in eyes with AMD, choroidal thickness was variable. This may be due to the fact that they used Cirrus SD-OCT, and only 38% of their sample could be imaged reliably and included in the study. In their study, eyes with AMD on average had a thinner choroid than that of normal controls. Furthermore, eyes with exudative AMD had thinner choroids than eyes with nonexudative AMD.<sup>42</sup> Switzer et al<sup>43</sup> explored the relationship between different phenotypes seen in early AMD and choroidal thickness. They reported that eyes with fundus tessellation,  $\beta$  zone peri-papillary atrophy, absence of conventional drusen, sub-retinal drusenoid deposits (SRDD), open angle glaucoma, or an absence of the contact cylinder band on SD-OCT had a thinner choroid than eyes without these features.<sup>43</sup>

Reticular pseudo-drusen or SRDD confers an increased risk for the development of late AMD.<sup>44</sup> The main finding of the histopathological examination of an eye with SRDD was the loss of the small choroidal vessels with an increased spacing between the large choroidal veins. The authors of this report proposed that the choroidal stroma was replaced by fibrous tissue in a reticular pattern.<sup>45</sup> Prior to EDI-OCT of the choroid, it was not possible to verify this hypothesis. Choroidal EDI-OCT has shown that eyes with SRDD appear to have a thinner choroid than eyes with early AMD.<sup>43,46</sup> In one study, interestingly enough, the choroid was thinner in all points tested, except superior to the fovea. Multimodality imaging showed that the areas of increased choroidal

thickness correlated with the physical presence of SRDD.<sup>46</sup> It may well be that in eyes with SRDD, initially there is a diffuse loss of small choroidal vessels which lead to choroidal thinning. Later, the choroidal stroma is replaced by fibrous tissue which leads to a relative choroidal thickening. This replacement occurs predominantly in the area of SRDD, which happens to be in the superior macula.<sup>46</sup> Given the cross-sectional nature of these studies, it remains unclear if choroidal thinning causes reticular pseudodrusen or the presence of pseudodrusen contributes to choroidal thinning.

In eyes with exudative AMD, the subfoveal choroidal thickness has been reported to be thinner than eyes with polypoidal choroidal vasculopathy (PCV).<sup>41,47–49</sup> One group of investigators went one step further and correlated choroidal hyperpermeability, as seen on ICGA, with choroidal thickness.<sup>47</sup> In this study, some eyes with exudative AMD exhibited choroidal hyperpermeability and some eyes did not have choroidal hyperpermeability. In patients with exudative AMD with choroidal hyperpermeability, subfoveal choroidal thickness did not differ between eyes with AMD and PCV. Conversely, in eyes with no choroidal hyperpermeability, the subfoveal choroidal thickness in eyes with PCV was significantly higher than that in eyes with AMD. In patients with unilateral disease, the fellow eyes had similar choroidal thickness as the involved eyes.<sup>47</sup> An association between the I62V polymorphism in the complement factor H (CFH) gene and choroidal thickness in eyes with PCV was identified in a Japanese study. Other polymorphisms such as the Y402H in the CFH gene and the A69S in the ARMS2 gene were not associated with subfoveal choroidal thickness. Since CFH regulates the alternative complement system, inflammation may play a role in the choroidal changes seen in PCV.<sup>47</sup>

The above findings suggest different underlying pathophysiological mechanisms between PCV and AMD. Two schools of thought regarding the pathogenesis of PCV currently exist. According to some, the choroidal vascular lesion seen in PCV is a variant of CNV.<sup>50</sup> Others propose that the choroidal vascular abnormalities seen in PCV are distinct from CNV.<sup>51</sup>

CSC and PCV are often difficult to differentiate from AMD, particularly in older patients. Since treatment for these conditions vary, it is important to make this distinction. Measuring the choroidal thickness may help differentiate between exudative AMD and PCV and between exudative AMD and CSC.<sup>41,47–49</sup> Both PCV and CSC eyes have thicker choroids than those in normal individuals. Conversely, eyes with exudative AMD have thinner choroids (Fig. 5). The distinction between CSC and PCV can be difficult at times, since they share many clinical and angiographic features. Yannuzzi et al<sup>52</sup> reported that patients with PCV may masquerade as CSC and recommended ICGA to differentiate between these conditions. Typical ICGA findings of PCV include a branching network of inner choroidal vessels with nodular aneurysmal hyperfluorescence at the edge of this vascular network.<sup>53</sup> ICGA has shown that eyes with PCV exhibit choroidal vascular hyperpermeability, which may result in an increased intrachoroidal hydrostatic pressure.<sup>30,54</sup> Similar ICGA choroidal vascular hyperpermeability findings have been described in eyes with CSC.<sup>30,54</sup> It is plausible that both PCV and CSC share common pathophysiological mechanisms. Recently, Ooto et al<sup>55</sup> used SD-OCT to show that the photoreceptor outer segments were much thinner in PCV eyes than those in CSC eyes.

The treatment effects on choroidal thickness remain unclear. In one study, eyes with exudative AMD that were treated with anti-VEGF agents had a trend towards thinner choroids when compared to treatment naive eyes.<sup>41</sup> In contrast, Jirarattanasopa et al<sup>47</sup> reported that choroidal thickness decreased in both PCV and AMD eyes if treated with a combination of verteporfin photodynamic therapy and intravitreal ranibizumab. Eyes treated

only with ranibizumab did not have a change in choroidal thickness. In another study, eyes with exudative AMD that were treated with intravitreal ranibizumab had a decrease in choroidal thickness.<sup>56</sup>

The pathogenesis of a pigment epithelial detachment (PED) associated with exudative AMD has been a subject of controversy for several years. On the one hand, Gass proposed that a PED arises from either serous exudation from choriocapillaris hyperpermeability through an intact Bruch's membrane or as a consequence of choroidal neovascularization (CNV) with secondary exudation directly into the sub-RPE space. On the other hand, Bird and Marshall<sup>57</sup> proposed that increasing lipid deposition into Bruch's membrane rendered it hydrophobic and blocked the normal passage of fluid.<sup>58,59</sup> The build-up of fluid would create a PED. Furthermore, they stated that if CNV occurred it would be as a consequence of the PED and not the other way around.<sup>57–59</sup> Part of the reason why it has been difficult to study the pathogenesis of PED is the fact that there are no adequate histopathological studies. In addition, imaging modalities such as OCT characteristically reveal an empty hyporeflective space in the internal structure of a serous PED. Given the limitations of conventional OCT choroidal imaging, it was unclear if the optically empty space was really optically empty or was filled with material that simply was not imaged due to its location deep down in the choroid. Spaide<sup>60</sup> used EDI-OCT to demonstrate that PEDs were often filled with material suggestive of choroidal neovascularization lending support to Gass's theory of neovascular origin for PEDs (Fig. 6). Coscas et al<sup>61</sup> have recently used en face EDI-OCT to image fibrovascular PED. They reported clear CNV visualization and localization within the fibrovascular PED.

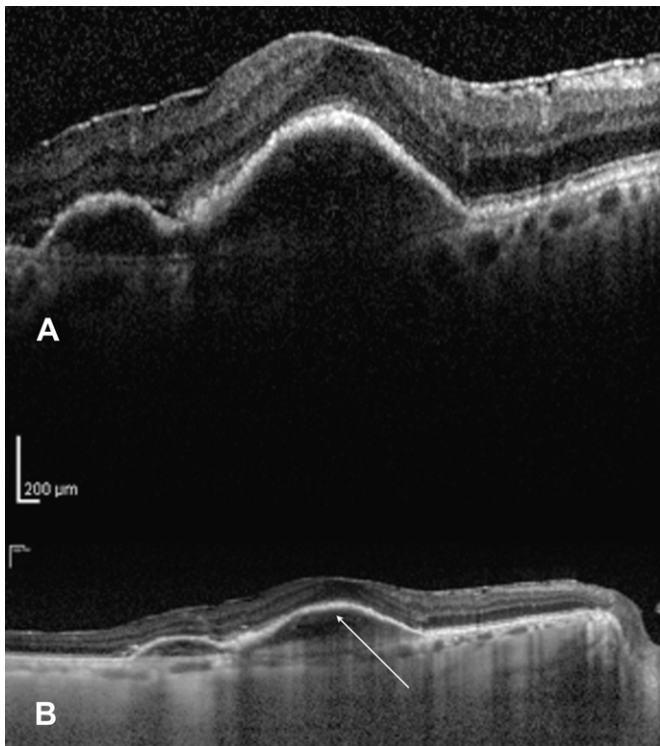


**Fig. 6.** Comparison between conventional Spectralis optical coherence tomography (OCT) scanning and enhanced depth imaging (EDI) OCT scanning of an eye with a pigment epithelial detachment (PED) associated with exudative age-related macular degeneration. (A). Conventional Spectralis OCT scanning. Note the optically empty area under the PED. (B). EDI Spectralis OCT imaging of the same patient. Note that the area under the PED is no longer optically empty suggesting neovascularization (arrow).

## 7. Age-related choroidal atrophy

Spaide<sup>62</sup> used EDI-OCT to describe a new clinical entity, age-related choroidal atrophy. In his cohort of 28 patients, the mean visual acuity was 20/40, the mean age was 80.6 years, and all eyes had a tessellated fundus appearance. Close to a third of the eyes suffered from concurrent late AMD. Glaucoma was present in over a third of the patients. The mean subfoveal choroidal thickness was only 70  $\mu\text{m}$ . The loss of choroidal thickness was associated with the loss of visible vessels, implying that age-related choroidal atrophy is a manifestation of small-vessel disease affecting the choroid.<sup>62</sup>

## 8. Vogt-Koyanagi-Harada Syndrome

The Vogt-Koyanagi-Harada (VKH) syndrome is characterized by an autoimmune response against melanin containing tissues. Since the choroid contains most of the melanocytes in the eye, it is often targeted in this condition. Eyes with acute disease exhibit a granulomatous choroidal inflammatory infiltrate that thickens the choroid.<sup>63</sup> Both ultrasonography and ICGA have been used to monitor response to therapy by assessing the choroid. Their main limitation is the inability to analyze the data in a quantitative fashion.

EDI-OCT measured choroidal thickness might be used longitudinally as a surrogate marker of disease activity in the Vogt-Koyanagi-Harada (VKH) syndrome.<sup>64–66</sup> Eyes with new onset acute disease manifest markedly increased choroidal thickness. Once the inflammation is brought under control, choroidal thickness decreases rapidly.<sup>64,66,67</sup> This decrease in choroidal thickness has been correlated with a decreasing height of the serous retinal detachment and visual improvement.<sup>64,67</sup> Choroidal thickness in excess of 550  $\mu\text{m}$  at 1 week after initiating treatment correlates with the development of peripapillary atrophy.<sup>67</sup> Peripapillary atrophy in VKH has been associated with retinal dysfunction and inadequate immunosuppressive therapy.<sup>68,69</sup> Nakayama et al<sup>67</sup> speculated that a thicker choroid represents a greater inflammatory burden that causes a greater tissue destruction acutely, resulting in a greater atrophy in the convalescent phase.

If a recurrence occurs, the choroid becomes thickened again.<sup>65,67</sup> During the convalescent stage, the mean choroidal thickness is thinner in VKH eyes than normal control eyes, particularly in eyes with a sunset glow fundus appearance.<sup>65</sup> A prospective case control study compared choroidal thickness in eyes with long standing VKH (defined as >6 months duration) with an aged control group.<sup>70</sup> The choroid was significantly thinner in eyes with VKH compared to normal controls. There was no difference in choroidal thickness in eyes with and without clinical inflammation, which is in stark difference to eyes with new onset acute disease. This chronic choroidal thinning is most likely the result of choroidal atrophy. EDI-OCT of the choroid has enabled observers to report a loss of focal hyperreflectivity in the inner choroid of eyes with VKH in both the acute and convalescent stages. These inner choroidal hyperreflective foci probably represent small choroidal vessels.<sup>66</sup> Their loss during the acute stage might be secondary to compression by granulomas and nonperfusion caused by the massive inflammatory infiltration. ICGA has shown filling delays of the choriocapillaris.<sup>71</sup> In an ICGA pathological correlation, hypoperfused black spots, presumed to be granulomas, were seen compressing the choriocapillaris.<sup>72</sup> During the convalescent stage, stromal scarring and loss of small vessel disease results in tissue loss, which is manifested as choroidal thinning.<sup>66</sup>

## 9. Macular holes

Idiopathic macular holes are thought to arise from abnormal vitreomacular traction.<sup>73</sup> Recent EDI-OCT studies have suggested



that the choroid might play a role in this condition.<sup>74,75</sup> In these studies, the subfoveal choroidal thickness of eyes with full thickness idiopathic macular hole were compared with the nonaffected fellow eye and controls. In general, subfoveal choroidal thickness in eyes with the macular hole and in the healthy fellow eye is thinner than control eyes. There was no correlation between subfoveal choroidal thickness and the diameter of the hole in one study.<sup>74</sup> In the other study, a trend was seen for a thinner choroid to be associated with a larger macular hole.<sup>75</sup> In contrast, Schaal et al<sup>76</sup> did not find any differences in choroidal thickness between eyes with macular hole and control eyes. These observations if real, suggest that bilateral thinning of the choroid may precede macular hole formation. Over 25 years ago, Morgan and Schatz<sup>77</sup> proposed that involutinal macular thinning was an important step in the pathogenesis of idiopathic macular hole. Given the cross-sectional nature of these studies, it remains unclear whether choroidal thinning is the result or the cause of idiopathic macular hole.

## 10. Inherited retinal diseases

Retinitis pigmentosa refers to a group of inherited disorders caused by multiple genetic defects that manifest progressive photoreceptor degeneration. In retinitis pigmentosa there is a marked reduction in choroidal blood flow and velocity, which correlates with disease severity.<sup>78,79</sup> Currently there is no treatment available. Among the experimental therapies being explored, visual prostheses are being studied as means to restore some visual function in end-stage eyes. In order to design appropriate supra-choroidal implants, accurate choroidal thickness measurements are needed in order to calculate the distance between the implant and the ganglion cell layer.<sup>80</sup>

On EDI-OCT patients with retinitis pigmentosa have significantly thinner choroids than normal individuals.<sup>81,82</sup> Ayton et al<sup>81</sup> reported that patients with the worse visual acuity and a longer history of symptoms had significantly thinner choroids. In contrast, Dhoot and colleagues<sup>82</sup> found that there was no correlation between visual acuity and choroidal thickness. They also reported choroidal thinning in eyes with relatively good visual acuity suggesting that choroidal blood flow abnormalities rather than photoreceptor degeneration are responsible for such thinning.

A retrospective observational case series consisting of 20 eyes with a variety of inherited retinal diseases such as Best disease, Stargardt, choroidemia, peripherin retinal degeneration slow (RDS) mutations, and Bietti crystalline retinal dystrophy reported that the degree of choroidal thinning depended on the underlying condition and also in the stage of the disease.<sup>83</sup> For instance, in early Stargardt disease, there was no choroidal thinning but in advanced cases choroidal thinning was present. The authors suggest that in diseases limited to the macula, focal choroidal thinning was probably secondary to choriocapillaris atrophy caused by RPE death. In contrast, as expected, diffuse choroidal thinning was seen in eyes with choroidemia. In this study, there was no correlation between choroidal thinning and visual acuity, extent of retinal dysfunction or electrophysiological findings.<sup>83</sup>

## 11. Diabetic retinopathy

Despite the fact that diabetes mellitus also affects the choroid,<sup>84</sup> little is known clinically about diabetic choroidopathy. Diabetic patients with diabetic retinopathy appear to have a thinner choroid.<sup>85–89</sup> However, it remains unclear if the degree or severity of diabetic retinopathy influences choroidal thickness. According to an observational comparative study that used the Nidek Retinascan RS 3000 SD-OCT (Gamagori, Japan), choroidal thickness was indirectly proportional to the degree of diabetic retinopathy. The

choroidal thickness in diabetic eyes without retinopathy did not differ from normal control eyes. In addition, there was no correlation observed between macular edema and choroidal thickness or between choroidal and retinal thickness.<sup>85</sup> In another study using Cirrus SD-OCT, there was no difference in choroidal thickness in eyes with nonproliferative diabetic retinopathy and normal control eyes. Interestingly, eyes with diabetic macular edema and treated eyes with proliferative diabetic retinopathy exhibited thinner choroids than their normal counterparts.<sup>87</sup> Querques et al<sup>86</sup> investigated the changes in macular choroidal thickness in a series of 63 diabetic eyes with the Spectralis SD-OCT. They compared diabetic eyes with no retinopathy, nonproliferative diabetic retinopathy with no macular edema and nonproliferative diabetic retinopathy with macular edema. They reported that there was no difference in the subfoveal choroidal thickness in the different diabetic groups. Since choroidal blood flow is compromised in diabetic patients,<sup>90</sup> Querques and colleagues<sup>86</sup> suggest that a decreased choroidal blood flow is related to the decrease in choroidal thickness. According to them, diabetes mellitus (DM) may cause choriocapillaris atrophy, which in turn leads to an increase in vascular resistance and a decrease in choriocapillaris blood flow. The impaired choriocapillaris blood flow may lead to macular hypoxia and vascular endothelial growth factor (VEGF) secretion, thus contributing to the pathogenesis of diabetic macular edema.<sup>86,87</sup> Three-dimensional 1060-nm OCT choroidal thickness maps revealed that the central and inferior choroid were thinner in diabetic eyes as compared to normal controls. In this study, choroidal thickness was also indirectly proportional to the degree of diabetic retinopathy. Diabetic eyes without retinopathy had similar choroidal thickness as the controls.<sup>88,89</sup> It remains unclear what causes choroidal thinning since the choroidal thinning exceeds the magnitude of choriocapillaris atrophy.<sup>88</sup> Choroidal EDI-OCT imaging might be an useful method to study the contribution of the choroidal circulation to the overall visual dysfunction seen in diabetic patients.

## 12. Glaucoma

The basic pathophysiological mechanisms of glaucoma remain unknown. According to one theory, glaucomatous optic nerve damage occurs as a result of an ischemic insult following a reduced blood flow at the level of the lamina cribrosa. Since the choroid is the intraocular tissue that carries the highest blood flow, there has been interest in studying what role if any the choroid might play in the pathogenesis of glaucoma.

Histopathological studies of autopsy eyes suggest that the choroid is thinner in glaucomatous eyes.<sup>91,92</sup> Yet *in vivo* studies with EDI-OCT have not substantiated these findings.<sup>93–96</sup> Mwanza and colleagues<sup>94</sup> have reported that the choroidal thickness as measured with EDI-OCT is similar among normal, normal tension glaucoma and primary open angle glaucoma eyes. Similar findings were reported by Fenolland et al.<sup>95</sup> Arora et al<sup>97</sup> did not find any significant differences in choroidal thickness between eyes with open angle glaucoma and normal controls. Maul et al<sup>93</sup> reported that choroidal thickness did not differ in eyes with glaucoma and eyes that were suspicious for glaucoma. Furthermore, no correlation between choroidal thickness and glaucoma damage could be documented.<sup>93,96</sup> Central corneal thickness and diastolic perfusion pressure are variables that affect choroidal thickness in glaucoma and glaucoma suspect eyes.<sup>93</sup>

The choroid is thicker in angle closure than in open angle and control eyes.<sup>97</sup> Rapid drinking of 1 L of water over 30 minutes induces significant increases in intraocular pressure and choroidal thickness in eyes with angle closure glaucoma. This may signify that in eyes with angle closure, the choroid has a greater tendency

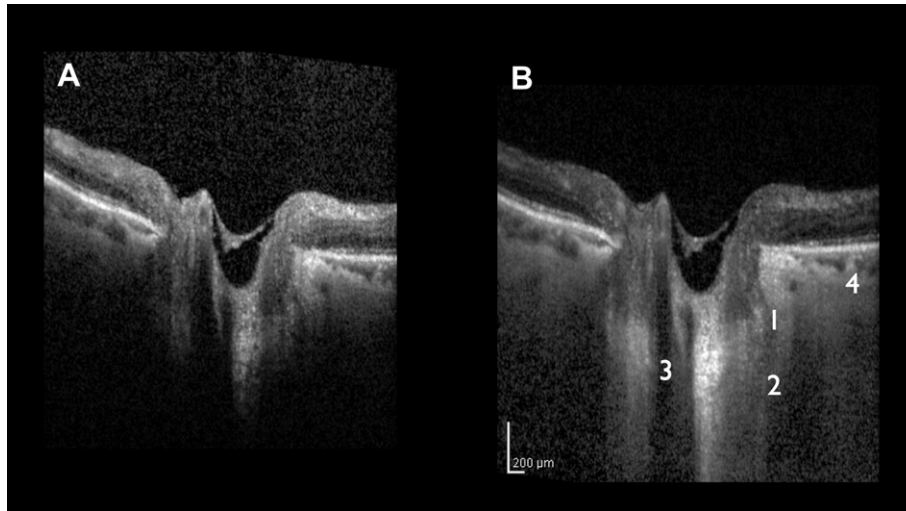


**Fig. 7.** Comparison between conventional Spectralis optical coherence tomography (OCT) scanning and enhanced depth imaging (EDI) OCT scanning of the optic nerve of the same patient. (A) Conventional OCT of the optic nerve region. (B) EDI-OCT of the same patient demonstrating better detail of the lamina cribrosa and adjacent structures. 1 = anterior border of the lamina cribrosa; 2 = posterior border of the lamina cribrosa; 3 = central retinal vein; 4 = choriocleral junction.

to expand.<sup>98</sup> Based on these findings, Arora et al<sup>97</sup> hypothesized that the increased intraocular volume secondary to choroidal expansion leads to an immediate increase in intraocular pressure. As a compensatory mechanism, aqueous outflow across the trabecular meshwork increases to try to restore normal intraocular pressure. As fluid leaves the anterior chamber, the aqueous volume of the anterior chamber diminishes, creating a posterior to anterior pressure gradient. As a result, the lens moves forward, making the iris lens channel narrower and increasing resistance to pupillary aqueous flow. At the same time, the iris bows forward and occludes the trabecular meshwork. Thus, in eyes with a narrow angle, dynamic choroidal expansion may contribute to angle closure.

In addition biomechanical factors such as the translaminal pressure gradient (TLPG) and the translaminal pressure difference (defined as intraocular pressure minus the cerebrospinal fluid pressure) may contribute to optic nerve injury in glaucoma. An elevated TLPG blocks axoplasmic flow across the lamina cribrosa, causing axonal injury.<sup>99</sup> The translaminal pressure difference has been associated to neuroretinal rim area and visual field defect.<sup>100</sup> The TLPG is directly related to the translaminal pressure difference and inversely related to the lamina cribrosa thickness.<sup>101</sup>

EDI-OCT imaging has allowed the *in vivo* study of the human optic nerve head and surrounding structures such as the lamina cribrosa, short posterior ciliary arteries, central retinal artery, central retinal vein, the peripapillary choroid, peripapillary sclera, and the subarachnoid space around the optic nerve.<sup>102,103</sup> (Fig. 7) The central retinal vein and artery were seen in all eyes. In high myopia, the subarachnoid space around the optic nerve may also be imaged. The lamina cribrosa was well identified in most eyes. Its anterior surface was seen in part in all eyes, whereas the pores were detected in over three-fourths of eyes. Given the difficulty in imaging the posterior border of the lamina cribrosa, Lee and colleagues<sup>101</sup> have proposed using thin slab maximum intensity projection image to improve the reproducibility of the lamina cribrosa EDI-OCT measurements.

EDI-OCT imaging of the human optic nerve head may prove to be useful in studying the pathogenesis of glaucoma.<sup>102,103</sup> In a group of healthy individuals, the thickness of the central lamina cribrosa correlated with age but did not correlate with axial length or central corneal thickness.<sup>104</sup> It appears that the lamina cribrosa is thinner in glaucomatous eyes when compared to glaucoma suspects or normal controls.<sup>102,105</sup> A recent study demonstrated that an

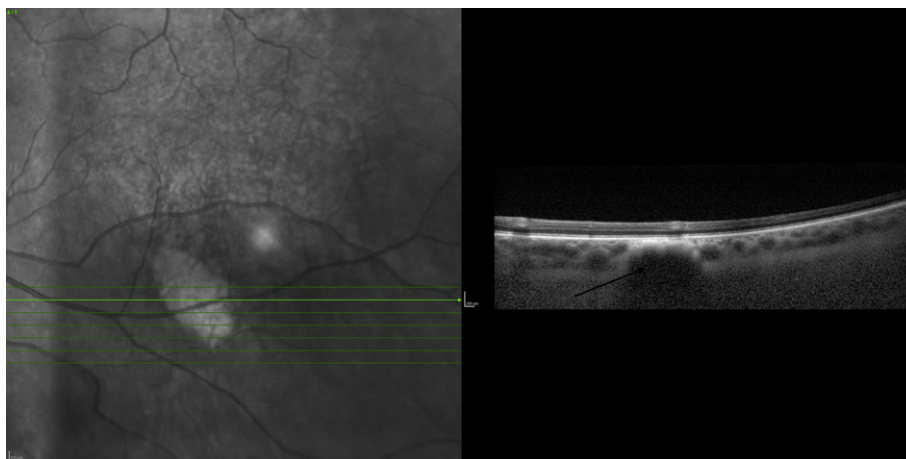


**Fig. 8.** Enhanced depth imaging of a choroidal nevus. Note the hyper-reflective band within the choriocapillaris with posterior shadowing.



acute increase in intraocular pressure did not cause much of a displacement in the lamina cribrosa of glaucomatous eyes or normal control eyes.<sup>106</sup> In contrast, glaucomatous eyes that underwent surgical intervention to reduce intraocular pressure, manifested anterior lamellar displacement and thickening of the prelaminar tissue.<sup>107</sup> These different findings have been attributed to the differences in intraocular pressure change and duration plus the differences in the study populations.<sup>108</sup>

### 13. Tumors

Small choroidal tumors located in the posterior pole that are not detectable by ultrasound may be imaged and studied by EDI-OCT<sup>109</sup> (Fig. 8). In contrast, larger tumors (>1 mm in height or >9 mm in diameter) are not appropriate for EDI-OCT since the borders of the tumors fall beyond the boundaries of the instrument. Certain characteristic features have been described. Both melanomas and choroidal nevi had a highly reflected band within the choriocapillaris that caused posterior shadowing of the underlying structures. The presence of choroidal vascular spaces of normal caliber differentiates a nevus from a melanoma. In a retrospective comparative study of choroidal nevi and small choroidal melanoma, Shields et al<sup>110</sup> demonstrated that ultrasound overestimated tumor thickness by 55% in small choroidal melanoma. EDI-OCT features that differentiated small choroidal melanoma from choroidal nevi included increased tumor thickness, the presence of subretinal fluid, subretinal lipofuscin deposition, and retinal irregularities. EDI-OCT demonstrate that the majority of choroidal nevi have overlying choriocapillaris thinning<sup>111</sup> (Fig. 8).

An EDI-OCT with a low reflective band in the posterior choroid with enlargement of the suprachoroidal space suggests choroidal metastasis.<sup>109</sup> Circumscribed choroidal hemangiomas were characterized by a homogeneous signal of low to medium reflectivity with large intrinsic spaces.<sup>109</sup> Thus, EDI-OCT and ultrasound may serve as complementary ancillary exams in the management of posteriorly located choroidal tumors.

### 14. Conclusions

In summary, EDI-OCT is a reproducible technique that allows imaging of the choroid and deep optic nerve structures. Reproducible measurements of choroidal and lamina cribrosa thickness are possible. Several variables such as age, axial length and time of day affect choroidal thickness and must be taken into account when interpreting the data on choroidal thickness. Lamina cribrosa thickness appears to be affected by age as well but other factors need to be determined. Choroidal thickness may be used to differentiate between CSC, PCV, and exudative AMD. EDI-OCT of the choroid may detect tumors not detectable by ultrasound. Studying the choroid may help us gain insight into the pathogenesis of several diseases such as AMD, CSC, glaucoma, posteriorly located choroidal tumors, and PCV among others. Limitations of current techniques include the lack of automated segmentation software but improvements are in the horizon. We are just really beginning to explore the depths of the choroid and optic nerve. With improvements in technology, we can only imagine what the future will bring.

### References

1. Alm A, Bill A. Ocular and optic nerve blood flow at normal and increased intraocular pressures in monkeys (*Macaca irus*): a study with radioactively labelled microspheres including flow determinations in brain and some other tissues. *Exp Eye Res* 1973;**15**:15–29.
2. Huang D, Swanson EA, Lin CP, Schuman JS, Stinson WG, Chang W, et al. Optical coherence tomography. *Science* 1991;**254**:1178–81.

3. Hee MR, Izatt JA, Swanson EA, Huang D, Schuman JS, Lin CP, et al. Optical coherence tomography of the human retina. *Arch Ophthalmol* 1995;**113**:325–32.
4. Margolis R, Spaide RF. A pilot study of enhanced depth imaging optical coherence tomography of the choroid in normal eyes. *Am J Ophthalmol* 2009;**147**:811–5.
5. Spaide RF, Koizumi H, Pozzoni MC. Enhanced depth imaging spectral-domain optical coherence tomography. *Am J Ophthalmol* 2008;**146**:496–500.
6. Ikuno Y, Kawaguchi K, Nouchi T, Yasuno Y. Choroidal thickness in healthy Japanese subjects. *Invest Ophthalmol Vis Sci* 2010;**51**:2173–6.
7. Srinivasan VJ, Adler DC, Chen Y, Gorczynska I, Huber R, Duker JS. Ultrahigh-speed optical coherence tomography for three-dimensional and en face imaging of the retina and optic nerve head. *Invest Ophthalmol Vis Sci* 2008;**49**:5103–10.
8. Manjunath V, Taha M, Fujimoto JG, Duker JS. Choroidal thickness in normal eyes measured using Cirrus HD optical coherence tomography. *Am J Ophthalmol* 2010;**150**:325–9. e1.
9. Manjunath V, Fujimoto JG, Duker JS. Cirrus HD-OCT high definition imaging is another tool available for visualization of the choroid and provides agreement with the finding that the choroidal thickness is increased in central serous chorioretinopathy in comparison to normal eyes. *Retina* 2010;**30**:1320–1. author reply 1–2.
10. Lin P, Mettu PS, Pomerleau DL, Chiu SJ, Maldonado R, Stinnett S, et al. Image inversion spectral-domain optical coherence tomography optimizes choroidal thickness and detail through improved contrast. *Invest Ophthalmol Vis Sci* 2012;**53**:1874–82.
11. Zhang L, Lee K, Niemeijer M, Mullins RF, Sonka M, Abramoff MD. Automated Segmentation of the Choroid from Clinical SD-OCT. *Invest Ophthalmol Vis Sci* 2012;**53**:7510–9.
12. Ouyang Y, Heussen FM, Mokwa N, Walsh AC, Durbin MK, Keane PA, et al. Spatial distribution of posterior pole choroidal thickness by spectral domain optical coherence tomography. *Invest Ophthalmol Vis Sci* 2011;**52**:7019–26.
13. Rahman W, Chen FK, Yeoh J, Patel P, Tufail A, Da Cruz L. Repeatability of manual subfoveal choroidal thickness measurements in healthy subjects using the technique of enhanced depth imaging optical coherence tomography. *Invest Ophthalmol Vis Sci* 2011;**52**:2267–71.
14. Branchini L, Regatieri CV, Flores-Moreno J, Baumann B, Fujimoto JG, Duker JS. Reproducibility of choroidal thickness measurements across three spectral domain optical coherence tomography systems. *Ophthalmology* 2012;**119**:119–23.
15. Chhablani J, Barteselli G, Wang H, El-Emam S, Kozak I, Doede AL, et al. Repeatability and reproducibility of manual choroidal volume measurements using enhanced depth imaging optical coherence tomography. *Invest Ophthalmol Vis Sci* 2012;**53**:2274–80.
16. Ikuno Y, Maruko I, Yasuno Y, Miura M, Sekiryu T, Nishida K, et al. Reproducibility of retinal and choroidal thickness measurements in enhanced depth imaging and high-penetration optical coherence tomography. *Invest Ophthalmol Vis Sci* 2011;**52**:5536–40.
17. Fujiwara T, Imamura Y, Margolis R, Slakter JS, Spaide RF. Enhanced depth imaging optical coherence tomography of the choroid in highly myopic eyes. *Am J Ophthalmol* 2009;**148**:445–50.
18. Nishida Y, Fujiwara T, Imamura Y, Lima LH, Kurosaka D, Spaide RF. Choroidal thickness and visual acuity in highly myopic eyes. *Retina* 2012;**32**:1229–36.
19. Li XQ, Larsen M, Munch IC. Subfoveal choroidal thickness in relation to sex and axial length in 93 Danish university students. *Invest Ophthalmol Vis Sci* 2011;**52**:8438–41.
20. Chen FK, Yeoh J, Rahman W, Patel PJ, Tufail A, Da Cruz L. Topographic variation and interocular symmetry of macular choroidal thickness using enhanced depth imaging optical coherence tomography. *Invest Ophthalmol Vis Sci* 2012;**53**:975–85.
21. Sogawa K, Nagaoka T, Takahashi A, Tanano I, Tani T, Ishibazawa A, et al. Relationship between choroidal thickness and choroidal circulation in healthy young subjects. *Am J Ophthalmol* 2012;**153**:1129–32. e1.
22. Kim M, Kim SS, Kwon HJ, Koh HJ, Lee SC. Association between choroidal thickness and ocular perfusion pressure in young, healthy subjects: enhanced depth imaging optical coherence tomography study. *Invest Ophthalmol Vis Sci* 2012;**53**:7710–7.
23. Alwassia AA, Adhi M, Zhang JY, Regatieri CV, Al-Quthami A, Salem D, et al. Exercise-induced acute changes in systolic blood pressure do not alter choroidal thickness as measured by a portable spectral-domain optical coherence tomography device. *Retina* 2012;**33**:160–5.
24. Usui S, Ikuno Y, Miki A, Matsushita K, Yasuno Y, Nishida K. Evaluation of the choroidal thickness using high-penetration optical coherence tomography with long wavelength in highly myopic normal-tension glaucoma. *Am J Ophthalmol* 2012;**153**:10–6. e1.
25. Tan CS, Ouyang Y, Ruiz H, Sada SR. Diurnal variation of choroidal thickness in normal, healthy subjects measured by spectral domain optical coherence tomography. *Invest Ophthalmol Vis Sci* 2012;**53**:261–6.
26. McCourt EA, Cadena BC, Barnett CJ, Ciardella AP, Mandava N, Kahook MY. Measurement of subfoveal choroidal thickness using spectral domain optical coherence tomography. *Ophthalmic Surg Lasers Imaging* 2010;**41**:S28–33.
27. Guyer DR, Yannuzzi LA, Slakter JS, Sorenson JA, Ho A, Orlock D. Digital indocyanine green videoangiography of central serous chorioretinopathy. *Arch Ophthalmol* 1994;**112**:1057–62.

28. Imamura Y, Fujiwara T, Margolis R, Spaide RF. Enhanced depth imaging optical coherence tomography of the choroid in central serous chorioretinopathy. *Retina* 2009;**29**:1469–73.
29. Maruko I, Iida T, Sugano Y, Ojima A, Ogasawara M, Spaide RF. Subfoveal choroidal thickness after treatment of central serous chorioretinopathy. *Ophthalmology* 2010;**117**:1792–9.
30. Jirarattanasopa P, Ooto S, Tsujikawa A, Yamashiro K, Hangai M, Hirata M, et al. Assessment of macular choroidal thickness by optical coherence tomography and angiographic changes in central serous chorioretinopathy. *Ophthalmology* 2012;**119**:1666–78.
31. Pryds A, Larsen M. Choroidal thickness following extrafoveal photodynamic treatment with verteporfin in patients with central serous chorioretinopathy. *Acta Ophthalmol* 2011;**90**:738–43.
32. Kim YT, Kang SW, Bai KH. Choroidal thickness in both eyes of patients with unilaterally active central serous chorioretinopathy. *Eye (Lond)* 2011;**25**:1635–40.
33. Iida T, Kishi S, Hagimura N, Shimizu K. Persistent and bilateral choroidal vascular abnormalities in central serous chorioretinopathy. *Retina* 1999;**19**:508–12.
34. Vance SK, Imamura Y, Freund KB. The effects of sildenafil citrate on choroidal thickness as determined by enhanced depth imaging optical coherence tomography. *Retina* 2011;**31**:332–5.
35. Kim DY, Silverman RH, Chan RV, Khanifar AA, Rondeau M, Lloyd H, et al. Measurement of choroidal perfusion and thickness following systemic sildenafil (Viagra®). *Acta Ophthalmol* 2013;**91**:183–8.
36. Rosenbaum JT. Eyeing macular degeneration—few inflammatory remarks. *N Engl J Med* 2012;**367**:768–70.
37. Friedman E. A hemodynamic model of the pathogenesis of age-related macular degeneration. *Am J Ophthalmol* 1997;**124**:677–82.
38. Harris A, Chung HS, Ciulla TA, Kagemann L. Progress in measurement of ocular blood flow and relevance to our understanding of glaucoma and age-related macular degeneration. *Prog Retin Eye Res* 1999;**18**:669–87.
39. Broekhuysse RM. The lipid composition of aging sclera and cornea. *Ophthalmologica* 1975;**171**:82–5.
40. Wood A, Binns A, Margrain T, Drexler W, Povazay B, Esmaeelpour M, et al. Retinal and choroidal thickness in early age-related macular degeneration. *Am J Ophthalmol* 2011;**152**:1030–8. e2.
41. Chung SE, Kang SW, Lee JH, Kim YT. Choroidal thickness in polypoidal choroidal vasculopathy and exudative age-related macular degeneration. *Ophthalmology* 2011;**118**:840–5.
42. Manjunath V, Goren J, Fujimoto JG, Duker JS. Analysis of choroidal thickness in age-related macular degeneration using spectral-domain optical coherence tomography. *Am J Ophthalmol* 2011;**152**:663–8.
43. Switzer Jr DW, Mendonca LS, Saito M, Zweifel SA, Spaide RF. Segregation of ophthalmoscopic characteristics according to choroidal thickness in patients with early age-related macular degeneration. *Retina* 2012;**32**:1265–71.
44. Zweifel SA, Imamura Y, Spaide TC, Fujiwara T, Spaide RF. Prevalence and significance of subretinal drusenoid deposits (reticular pseudodrusen) in age-related macular degeneration. *Ophthalmology* 2010;**117**:1775–81.
45. Arnold JJ, Sarks SH, Killingsworth MC, Sarks JP. Reticular pseudodrusen. A risk factor in age-related maculopathy. *Retina* 1995;**15**:183–91.
46. Querques G, Querques L, Forte R, Massamba N, Coscas F, Souied EH. Choroidal changes associated with reticular pseudodrusen. *Invest Ophthalmol Vis Sci* 2012;**53**:1258–63.
47. Jirarattanasopa P, Ooto S, Nakata I, Tsujikawa A, Yamashiro K, Oishi A, et al. Choroidal thickness, vascular hyperpermeability, and complement factor H in age-related macular degeneration and polypoidal choroidal vasculopathy. *Invest Ophthalmol Vis Sci* 2012;**53**:3663–72.
48. Kim SW, Oh J, Kwon SS, Yoo J, Huh K. Comparison of choroidal thickness among patients with healthy eyes, early age-related maculopathy, neovascular age-related macular degeneration, central serous chorioretinopathy, and polypoidal choroidal vasculopathy. *Retina* 2011;**31**:1904–11.
49. Koizumi H, Yamagishi T, Yamazaki T, Kawasaki R, Kinoshita S. Subfoveal choroidal thickness in typical age-related macular degeneration and polypoidal choroidal vasculopathy. *Graefes Arch Clin Exp Ophthalmol* 2011;**249**:1123–8.
50. Uyama M, Matsubara T, Fukushima I, Matsunaga H, Iwashita K, Nagai Y, et al. Idiopathic polypoidal choroidal vasculopathy in Japanese patients. *Arch Ophthalmol* 1999;**117**:1035–42.
51. Yannuzzi LA, Ciardella A, Spaide RF, Rabb M, Freund KB, Orlock DA. The expanding clinical spectrum of idiopathic polypoidal choroidal vasculopathy. *Arch Ophthalmol* 1997;**115**:478–85.
52. Yannuzzi LA, Freund KB, Goldbaum M, Scarsellati-Sforzolini B, Guyer DR, Spaide RF, et al. Polypoidal choroidal vasculopathy masquerading as central serous chorioretinopathy. *Ophthalmology* 2000;**107**:767–77.
53. Spaide RF, Yannuzzi LA, Slakter JS, Sorenson J, Orlach DA. Indocyanine green videoangiography of idiopathic polypoidal choroidal vasculopathy. *Retina* 1995;**15**:100–10.
54. Sasahara M, Tsujikawa A, Musashi K, Gotoh N, Otani A, Mandai M, et al. Polypoidal choroidal vasculopathy with choroidal vascular hyperpermeability. *Am J Ophthalmol* 2006;**142**:601–7.
55. Ooto S, Tsujikawa A, Mori S, Tamura H, Yamashiro K, Yoshimura N. Thickness of photoreceptor layers in polypoidal choroidal vasculopathy and central serous chorioretinopathy. *Graefes Arch Clin Exp Ophthalmol* 2010;**248**:1077–86.
56. Yamazaki T, Koizumi H, Yamagishi T, Kinoshita S. Subfoveal choroidal thickness after ranibizumab therapy for neovascular age-related macular degeneration: 12-month results. *Ophthalmology* 2012;**119**:1621–7.
57. Bird AC, Marshall J. Retinal pigment epithelial detachments in the elderly. *Trans Ophthalmol Soc UK* 1986;**105**:674–82.
58. Moore DJ, Hussain AA, Marshall J. Age-related variation in the hydraulic conductivity of Bruch's membrane. *Invest Ophthalmol Vis Sci* 1995;**36**:1290–7.
59. Casswell AG, Kohlen D, Bird AC. Retinal pigment epithelial detachments in the elderly: classification and outcome. *Br J Ophthalmol* 1985;**69**:397–403.
60. Spaide RF. Enhanced depth imaging optical coherence tomography of retinal pigment epithelial detachment in age-related macular degeneration. *Am J Ophthalmol* 2009;**147**:644–52.
61. Coscas F, Coscas G, Querques G, Massamba N, Querques L, Bandello F, et al. En face enhanced depth imaging optical coherence tomography of fibrovascular pigment epithelium detachment. *Invest Ophthalmol Vis Sci* 2012;**53**:4147–51.
62. Spaide RF. Age-related choroidal atrophy. *Am J Ophthalmol* 2009;**147**:801–10.
63. Rao NA. Pathology of Vogt-Koyanagi-Harada disease. *Int Ophthalmol* 2007;**27**:81–5.
64. Maruko I, Iida T, Sugano Y, Oyama H, Sekiryu T, Fujiwara T, et al. Subfoveal choroidal thickness after treatment of Vogt-Koyanagi-Harada disease. *Retina* 2011;**31**:510–7.
65. Nakai K, Gomi F, Ikuno Y, Yasuno Y, Nouchi T, Ohguro N, et al. Choroidal observations in Vogt-Koyanagi-Harada disease using high-penetration optical coherence tomography. *Graefes Arch Clin Exp Ophthalmol* 2012;**250**:1089–95.
66. Fong AH, Li KK, Wong D. Choroidal evaluation using enhanced depth imaging spectral-domain optical coherence tomography in Vogt-Koyanagi-Harada disease. *Retina* 2011;**31**:502–9.
67. Nakayama M, Keino H, Okada AA, Watanabe T, Taki W, Inoue M, et al. Enhanced depth imaging optical coherence tomography of the choroid in Vogt-Koyanagi-Harada disease. *Retina* 2012;**32**:2061–9.
68. Chee SP, Luu CD, Cheng CL, Lim WK, Jap A. Visual function in Vogt-Koyanagi-Harada patients. *Graefes Arch Clin Exp Ophthalmol* 2005;**243**:785–90.
69. Jap A, Luu CD, Yeo I, Chee SP. Correlation between peripapillary atrophy and corticosteroid therapy in patients with Vogt-Koyanagi-Harada disease. *Eye (Lond)* 2008;**22**:240–5.
70. da Silva FT, Sakata VM, Nakashima A, Hirata CE, Olivales E, Takahashi WY, et al. Enhanced depth imaging optical coherence tomography in long-standing Vogt-Koyanagi-Harada disease. *Br J Ophthalmol* 2012;**97**:70–4.
71. Bouchenaki N, Herbert CP. The contribution of indocyanine green angiography to the appraisal and management of Vogt-Koyanagi-Harada disease. *Ophthalmology* 2001;**108**:54–64.
72. Herbert CP, Mantovani A, Bouchenaki N. Indocyanine green angiography in Vogt-Koyanagi-Harada disease: angiographic signs and utility in patient follow-up. *Int Ophthalmol* 2007;**27**:173–82.
73. Ho AC, Guyer DR, Fine SL. Macular hole. *Surv Ophthalmol* 1998;**42**:393–416.
74. Reibaldi M, Boscia F, Avitabile T, Uva MG, Russo V, Zagari M, et al. Enhanced depth imaging optical coherence tomography of the choroid in idiopathic macular hole: A cross-sectional prospective study. *Am J Ophthalmol* 2011;**151**:112–7. e2.
75. Zeng J, Li J, Liu R, Chen X, Pan J, Tang S, et al. Choroidal thickness in both eyes of patients with unilateral idiopathic macular hole. *Ophthalmology* 2012;**119**:2328–33.
76. Schaal KB, Pollithy S, Dithmar S. [Is choroidal thickness of importance in idiopathic macular hole?]. *Ophthalmologie* 2012;**109**:364–8.
77. Morgan CM, Schatz H. Involuntary macular thinning. A pre-macular hole condition. *Ophthalmology* 1986;**93**:153–61.
78. Falsini B, Anselmi GM, Marangoni D, D'Esposito F, Fadda A, Di Renzo A, et al. Subfoveal choroidal blood flow and central retinal function in retinitis pigmentosa. *Invest Ophthalmol Vis Sci* 2011;**52**:1064–9.
79. Langham ME, Kramer T. Decreased choroidal blood flow associated with retinitis pigmentosa. *Eye (Lond)* 1990;**4**:374–81.
80. Shivdasani MN, Luu CD, Cicione R, Fallon JB, Allen PJ, Leuenberger J, et al. Evaluation of stimulus parameters and electrode geometry for an effective suprachoroidal retinal prosthesis. *J Neural Eng* 2010;**7**:036008.
81. Ayton LN, Guymer RH, Luu CD. Choroidal thickness profiles in retinitis pigmentosa. *Clin Experiment Ophthalmol* 2012. Sep 7. <http://dx.doi.org/10.1111/j.1442-9071.2012.02867.x>. [Epub ahead of print].
82. Dhoot DS, Huo S, Yuan A, Xu D, Srivastava S, Ehlers JP, et al. Evaluation of choroidal thickness in retinitis pigmentosa using enhanced depth imaging optical coherence tomography. *Br J Ophthalmol* 2012;**97**:66–9.
83. Yeoh J, Rahman W, Chen F, Hooper C, Patel P, Tufail A, et al. Choroidal imaging in inherited retinal disease using the technique of enhanced depth imaging optical coherence tomography. *Graefes Arch Clin Exp Ophthalmol* 2010;**248**:1719–28.
84. Hidayat AA, Fine BS. Diabetic choroidopathy. Light and electron microscopic observations of seven cases. *Ophthalmology* 1985;**92**:512–22.
85. Vujosevic S, Martini F, Cavarzeran F, Pilotto E, Midena E. Macular and peripapillary choroidal thickness in diabetic patients. *Retina* 2012;**32**:1781–90.
86. Querques G, Lattanzio R, Querques L, Del Turco C, Forte R, Pierrro L, et al. Enhanced depth imaging optical coherence tomography in type 2 diabetes. *Invest Ophthalmol Vis Sci* 2012;**53**:6017–24.

87. Regatieri CV, Branchini L, Carmody J, Fujimoto JG, Duker JS. Choroidal thickness in patients with diabetic retinopathy analyzed by spectral-domain optical coherence tomography. *Retina* 2012;**32**:563–8.
88. Esmaeelpour M, Povazay B, Hermann B, Hofer B, Kajic V, Hale SL, et al. Mapping choroidal and retinal thickness variation in type 2 diabetes using three-dimensional 1060-nm optical coherence tomography. *Invest Ophthalmol Vis Sci* 2011;**52**:5311–6.
89. Esmaeelpour M, Brunner S, Shahrezaei SA, Nemetz S, Povazay B, Kajic V, et al. Choroidal thinning in diabetes type 1 detected by 3-dimensional 1060 nm optical coherence tomography. *Invest Ophthalmol Vis Sci* 2012;**53**:6803–9.
90. Nagaoka T, Kitaya N, Sugawara R, Yokota H, Mori F, Hikichi T, et al. Alteration of choroidal circulation in the foveal region in patients with type 2 diabetes. *Br J Ophthalmol* 2004;**88**:1060–3.
91. Kubota T, Jonas JB, Naumann GO. Decreased choroidal thickness in eyes with secondary angle closure glaucoma. An aetiological factor for deep retinal changes in glaucoma? *Br J Ophthalmol* 1993;**77**:430–2.
92. Yin ZQ, Vaegan Millar TJ, Beaumont P, Sarks S. Widespread choroidal insufficiency in primary open-angle glaucoma. *J Glaucoma* 1997;**6**:23–32.
93. Maul EA, Friedman DS, Chang DS, Boland MV, Ramulu PY, Jampel HD, et al. Choroidal thickness measured by spectral domain optical coherence tomography: factors affecting thickness in glaucoma patients. *Ophthalmology* 2011;**118**:1571–9.
94. Mwanza JC, Hochberg JT, Banitt MR, Feuer WJ, Budenz DL. Lack of association between glaucoma and macular choroidal thickness measured with enhanced depth-imaging optical coherence tomography. *Invest Ophthalmol Vis Sci* 2011;**52**:3430–5.
95. Fenolland JR, Giraud JM, May F, Mouinga A, Seck S, Renard JP. [Enhanced depth imaging of the choroid in open-angle glaucoma: A preliminary study]. *J Fr Ophtalmol* 2011;**34**:313–7.
96. Mwanza JC, Sayyad FE, Budenz DL. Choroidal thickness in unilateral advanced glaucoma. *Invest Ophthalmol Vis Sci* 2012;**53**:6695–701.
97. Arora KS, Jefferys JL, Maul EA, Quigley HA. The choroid is thicker in angle closure than in open angle and control eyes. *Invest Ophthalmol Vis Sci* 2012;**53**:7813–8.
98. Arora KS, Jefferys JL, Maul EA, Quigley HA. Choroidal thickness change after water drinking is greater in angle closure than in open angle eyes. *Invest Ophthalmol Vis Sci* 2012;**53**:6393–402.
99. Anderson DR, Hendrickson A. Effect of intraocular pressure on rapid axoplasmic transport in monkey optic nerve. *Invest Ophthalmol* 1974;**13**:771–83.
100. Ren R, Wang N, Zhang X, Cui T, Jonas JB. Trans-lamina cribrosa pressure difference correlated with neuroretinal rim area in glaucoma. *Graefes Arch Clin Exp Ophthalmol* 2011;**249**:1057–63.
101. Lee EJ, Kim TW, Weinreb RN. Improved reproducibility in measuring the lamina thickness on enhanced depth imaging SD-OCT images using maximum intensity projection. *Invest Ophthalmol Vis Sci* 2012;**53**:7576–82.
102. Lee EJ, Kim TW, Weinreb RN, Park KH, Kim SH, Kim DM. Visualization of the lamina cribrosa using enhanced depth imaging spectral-domain optical coherence tomography. *Am J Ophthalmol* 2011;**152**:87–95.e1.
103. Park SC, De Moraes CG, Teng CC, Tello C, Liebmann JM, Ritch R. Enhanced depth imaging optical coherence tomography of deep optic nerve complex structures in glaucoma. *Ophthalmology* 2012;**119**:3–9.
104. Lee EJ, Kim TW, Weinreb RN, Suh MH, Kim H. Lamina cribrosa thickness is not correlated with central corneal thickness or axial length in healthy eyes: central corneal thickness, axial length, and lamina cribrosa thickness. *Graefes Arch Clin Exp Ophthalmol* 2012. Sep 20. [Epub ahead of print].
105. Park HY, Jeon SH, Park CK. Enhanced depth imaging detects lamina cribrosa thickness differences in normal tension glaucoma and primary open-angle glaucoma. *Ophthalmology* 2012;**119**:10–20.
106. Agoumi Y, Sharpe GP, Hutchison DM, Nicoleta MT, Artes PH, Chauhan BC. Laminal and prelaminar tissue displacement during intraocular pressure elevation in glaucoma patients and healthy controls. *Ophthalmology* 2011;**118**:52–9.
107. Reis AS, O'Leary N, Stanfield MJ, Shuba LM, Nicoleta MT, Chauhan BC. Laminal displacement and prelaminar tissue thickness change after glaucoma surgery imaged with optical coherence tomography. *Invest Ophthalmol Vis Sci* 2012;**53**:5819–26.
108. Lee EJ, Kim TW, Weinreb RN. Reversal of lamina cribrosa displacement and thickness after trabeculectomy in glaucoma. *Ophthalmology* 2012;**119**:1359–66.
109. Torres VL, Brugnoli N, Kaiser PK, Singh AD. Optical coherence tomography enhanced depth imaging of choroidal tumors. *Am J Ophthalmol* 2011;**151**:586–93. e2.
110. Shields CL, Kaliki S, Rojanaporn D, Ferenczy SR, Shields JA. Enhanced depth imaging optical coherence tomography of small choroidal melanoma: comparison with choroidal nevus. *Arch Ophthalmol* 2012;**130**:850–6.
111. Shah SU, Kaliki S, Shields CL, Ferenczy SR, Harmon SA, Shields JA. Enhanced depth imaging optical coherence tomography of choroidal nevus in 104 cases. *Ophthalmology* 2012;**119**:1066–72.